A mixed, scalable domain decomposition method for incompressible flow

Etienne Vergnault[1,2], Olivier Allix[1], Serge Maison-le-Poëc[2]

[1] *LMT-Cachan (ENS Cachan/CNRS/UPMC/PRES UniverSud Paris)*
61 av. du Président Wilson, F-94230 Cachan, France
[2] *EADS Innovation Works*
12 rue Pasteur BP 76 F-92152 Suresnes, France
e-mail: vergnault@lmm.jussieu.fr, allix@lmt.ens-cachan.fr, serge.maison-le-poec@eads.net

This work deals with the construction of a mixed and extensible domain decomposition method for incompressible flows. In the scheme proposed here, the solution is sought at the intersection of two spaces, one containing the solution of the Navier–Stokes equations considered separately in each subdomain, and the other one containing the solutions of the compatibility equations on the interfaces. A solution verifying all the equations of the two spaces is achieved iteratively. One difficulty is that the interface problem is large and dense. In order to reduce its cost while maintaining the extensibility of the method, we defined an interface macroproblem in terms of a few interface macro unknowns. The best option takes advantage of the incompressibility condition to prescribe an interface macroproblem which propagates the information to the whole domain by making use of only two unknowns per interface. Several examples are used to illustrate the main properties of the method.

Keywords: Navier–Stokes, Domain Decomposition Method, Multiscale Method.

1. INTRODUCTION

This paper reports a first step towards the simulation of fluid-structure interaction (FSI) problems up to a failure using multiscale domain decomposition methods (e.g., FETI [5], BDD [13] or LaTIN [11]). The latter approach is already used for the simulation of damage in laminates under prescribed external loads [10]. In order to deal with fluid-structure interaction problems, we seek an extension of this method to fluid mechanics and FSI problems. Considering this particular context, and in this first development, we consider a pure fluid problem and undertake its resolution using a mixed, scalable domain decomposition approach. We use a fixed discretization within the framework of the Finite Element Method (FEM). The question of how FSI can be handled within this framework is the subject of a separate study [22].

The numerical resolution of fluid flow problems using the finite element method has been extensively investigated (see reference books such as [4, 23, and references therein].) For this study, in order to avoid re-meshing, we use a Eulerian description of the problem. Domain decomposition methods for fluid flows have been developed by many authors [1, 14, 16, 17]. In the framework of the FETI approach [5], Toselli [19] describes a method for scalar advection-diffusion equations. In that paper, single-level and dual-level FETI methods are applied to linear convection-dominated problems. The preconditioned nonsymmetrical condensed problem is solved by a GMRes algorithm. Li, in [12], adapts FETI algorithms to incompressible Stokes equations and proposed as primal-, dual- and dual-primal algorithms. There are further extensions to the linearised Navier–Stokes incompressible equations and nonlinear stationary incompressible flow problems using a Picard (fixed-point) iteration to deal with the convective nonlinear terms. In the present study, the non-linearity arising from the convective term of the Navier–Stokes equations is treated at the subdomain level,

instead of being linearised at the global level. FETI type methods are based on the elimination of the subdomain's degrees of freedom to obtain an interface problem usually solved by a conjugate gradient method. This type of method has been applied to incompressible flows by Vereecke et al. [21] and Glowinski et al. [6]. A mathematical study of non-overlapping domain decomposition method for the steady Navier–Stokes equations is available in [2].

Multigrid (MG) methods, (see, *e.g.*, [20]) have, among many other uses, been applied to flow problems. Two parallelized multigrid methods for viscous compressible flow were proposed in [3]; one results from the direct parallelization of multigrid operations, and the other is based on a Schwarz domain decomposition of the continuous problem and uses the multigrid algorithm as a solver for local systems. The hybrid DDM/MG method appears to be less efficient than direct parallelization.

The Variational MultiScale (VMS) method was initially proposed by Hughes et al. in [9] and applied to incompressible flows in [7]. The introduction of a supplementary micro-scale unknown enables a modeling of the so-called unsolvable small scales in the dynamic of the problem. Their effect is condensed on the macro-scale that corresponds to the finite element discretization, improving the quality of the solution. This method is dedicated to taking into account small-scale (*i.e.*, smaller than the mesh size) phenomena such as turbulence.

The reference incompressible flow problem, presented in Sec. 2, is solved by the finite element method on a Eulerian grid, with SUPG and PSPG stabilization. The computational domain is divided into subdomains and interfaces; the key ingredients of this mixed domain decomposition strategy are presented in Sec. 3. The decomposed problem is solved iteratively in Sec. 4. Then, the introduction, at a negligible extra cost, of a scale separation and a macroproblem enables us to accelerate the iterative resolution. In Sec. 5, two options for the implementation of the macroproblem are proposed, with different efficiencies. Section 6 presents numerical illustrations.

2. Problem statement

Let us consider an unsteady homogenous incompressible flow of a viscous fluid occupying a domain Ω bounded by $\partial\Omega$. The flow is subjected to a Dirichlet boundary condition $\underline{v}_d$ over $\partial_v\Omega$, to external surface forces $\underline{f}$ over $\partial_f\Omega = \partial\Omega \backslash \partial_v\Omega$, and to body forces $\underline{b}$ (e.g., gravity). The problem is formulated using velocity and pressure variables $\underline{v}$ and p, and is governed by mass and momentum conservation equations with a Newtonian material law.

2.1. The problem to be solved

The mass and momentum conservation equations along with the material law and the boundary and initial conditions form the complete set of the Navier–Stokes equations:

- The conservation of mass implies that the mass of a volume which follows the flow remains constant. The incompressibility hypothesis allows to write:

$$\underline{\nabla} \cdot \underline{v} = 0 \quad \text{in } \Omega.$$

- The conservation of momentum states the equilibrium between the acceleration and the applied and internal forces:

$$\rho \frac{\partial \underline{v}}{\partial t} + (\rho \underline{v} \cdot \underline{\nabla})\underline{v} = \underline{\nabla} \cdot \underline{\underline{\sigma}} + \rho \underline{b} \quad \text{in } \Omega, \tag{1}$$

where $\underline{\underline{\sigma}}$ is the Cauchy stress tensor and ρ is the density.

- Material law: for a Newtonian fluid under incompressible flow, the Cauchy stress is related to the velocity and pressure by

$$\underline{\underline{\sigma}} = -p\underline{\underline{I}} + \underline{\underline{\sigma}}_D = -p\underline{\underline{I}} + 2\mu\underline{\underline{\nabla}}^S \underline{v}, \tag{2}$$

where μ is the dynamic viscosity and $\underline{\underline{\sigma}}_D$ is the deviatoric stress tensor. $\underline{\underline{\nabla}}^S$ is the symmetric part of the gradient operator.

- Dirichlet boundary condition: over part of the domain's boundary, the flow is subjected to a prescribed velocity:

$$\underline{v} = \underline{v}_d \quad \text{over} \;\; \partial_{\underline{v}}\Omega.$$

Note that if $\partial_{\underline{v}}\Omega = \partial\Omega$, then $\underline{v}_d$ must be compatible with the incompressibility condition.

- Neumann boundary condition: over the complementary part of the boundary, the flow is subjected to a prescribed traction:

$$-p\underline{n} + 2\mu\underline{\underline{\nabla}}^S\underline{v} \cdot \underline{n} = \underline{f} \quad \text{over} \;\; \partial_{\underline{f}}\Omega. \tag{3}$$

- Initial condition: an unsteady flow develops from a given initial configuration:

$$\underline{v}(t=0) = \underline{v}_o.$$

Note that $\underline{v}_o$ must be divergence-free and that no initial condition for the pressure is needed. As the flow is assumed incompressible, the density is constant and Eqs. (1), (2) and (3) can be divided by ρ. In order to keep notations light, from now on, p will be the kinematic pressure that is the dynamic one divided by density, ν is the kinematic viscosity and $\underline{f}$ will designate the external prescribed forces divided by density:

$$\frac{\partial \underline{v}}{\partial t} + (\underline{v} \cdot \underline{\nabla})\underline{v} = \underline{\nabla} \cdot \underline{\underline{\sigma}}/\rho + \underline{b},$$

$$\underline{\underline{\sigma}}/\rho = -p\underline{\underline{I}} + 2\nu\underline{\underline{\nabla}}^S\underline{v},$$

$$- p\underline{n} + 2\nu\underline{\underline{\nabla}}^S\underline{v} \cdot \underline{n} = \underline{f}.$$

2.2. Weak form of the Navier–Stokes equations

Admissibility spaces. The trial solutions and weighting functions $(\underline{v}, \underline{w})$ and (p, q) are sought in the following spaces:

$$\underline{v} \in \mathscr{V}_d = (H^1(\Omega), \underline{v} = \underline{v}_d \;\; \text{over} \;\; \partial_{\underline{v}}\Omega) \times [0, T],$$

$$\underline{w} \in \mathscr{V}_0 = (H^1(\Omega), \underline{v} = \underline{0} \;\; \text{over} \;\; \partial_{\underline{v}}\Omega) \times [0, T],$$

$$p, q \in \mathscr{Q} = L^2(\Omega) \times [0, T].$$

In the case of a Dirichlet condition over the whole boundary $\partial\Omega$, p is defined to within an arbitrary constant which is removed by imposing an additional condition, such as having zero average or being zero at a given point. The corresponding trial solution space is then $\mathscr{Q}_0 = (L^2(\Omega)/\mathbb{R}) \times [0, T]$.

After integration by parts, on a fixed grid (Eulerian form), the weak form of the Navier–Stokes problem becomes:

Find $(\underline{v}, p) \in \mathscr{V}_d \times \mathscr{Q}$ such that $\forall(\underline{w}, q) \in \mathscr{V}_0 \times \mathscr{Q}$:

$$\left(\underline{w}, \underline{v}\underline{\nabla}\underline{v}\right)_\Omega + \left(\underline{\nabla}\underline{w}, 2\nu\underline{\underline{\nabla}}^S\underline{v}\right)_\Omega - \left(p, \underline{\nabla} \cdot \underline{w}\right)_\Omega - \left(q, \underline{\nabla} \cdot \underline{v}\right)_\Omega = \left(\underline{b}, \underline{w}\right)_\Omega + \left(\underline{f}, \underline{w}\right)_{\partial_{\underline{f}}\Omega}, \tag{4}$$

---

where $(\square, \diamondsuit)_\Omega$ denotes $\int_\Omega \square \cdot \diamondsuit \, \mathrm{d}\Omega$ and $(\square, \diamondsuit)_{\partial_{\underline{f}}\Omega}$ is $\int_{\partial_{\underline{f}}\Omega} \square \cdot \diamondsuit \, \mathrm{d}S$. Note that Eq. (4) has been obtained through what is called the velocity-stress divergence form of the momentum equation and thus $\underline{f}$ are boundary tractions. Let us rewrite the equation in a more compact form:

$$\mathscr{A}_\Omega(\underline{v}, \underline{w}, p, q) = (\underline{b}, \underline{w})_\Omega + \left(\underline{f}, \underline{w}\right)_{\partial_{\underline{f}}\Omega}. \tag{5}$$

2.3. Finite element discretization

Admissibility spaces. The Galerkin formulation of the Navier–Stokes problem leads to a mixed finite element system of equations. Let $\mathscr{V}_d^h$, $\mathscr{V}_0^h$ and $\mathscr{Q}^h$ denote finite-dimension subspaces of $\mathscr{V}_d$, $\mathscr{V}_0$ and $\mathscr{Q}$.

Stabilization. The Galerkin finite element method applied to the momentum equation leads to a central approximation of the convective term $(\underline{v}\underline{\nabla}\underline{v})$ and becomes unstable when convection dominates over diffusion. Using standard SUPG stabilization (See, *e.g.*, [4]), we modify the weak form Eq. (5) by adding a weighted residual (6) of the momentum equation:

$$\mathscr{R}(\underline{v},p) = \frac{\partial \underline{v}}{\partial t} + \underline{v}\underline{\nabla}\underline{v} - 2\nu\underline{\nabla}\cdot\underline{\underline{\nabla}}^S\underline{v} + \underline{\nabla}p - \underline{b}. \tag{6}$$

> Find $(\underline{v},p) \in \mathscr{V}_d^h \times \mathscr{Q}^h$ such that $\forall(\underline{w},q) \in \mathscr{V}_0^h \times \mathscr{Q}^h$:
> $$\mathscr{A}_\Omega^h(\underline{v},\underline{w},p,q) - (\underline{b},\underline{w})_\Omega - \left(\underline{f},\underline{w}\right)_{\partial\Omega} + \sum_{elements} \left(\tau_s\underline{v}\underline{\nabla}\underline{w} - \tau_p\underline{\nabla}q \ , \ \mathscr{R}(\underline{v},p)\right)_e = 0, \tag{7}$$

where τ_s is the SUPG stabilization parameter which, as proposed in [4], we set equal to

$$\tau_s = \left(\frac{1}{\theta\Delta t} + \frac{2||\underline{v}||}{h} + \frac{4\nu}{h^2}\right)^{-1},$$

where h is the local element size and $\theta = 1/2$ corresponds to time integration by trapezoidal rule.

Inf-sup condition. The shape functions for the interpolation of velocities and pressures must be chosen carefully because inappropriate choices would lead to an unstable solution. We use linear shape functions for velocities and pressures, leading to an element which is not *inf-sup* stable [4]. We add a PSPG stabilization term in Eq. (7), as proposed in [18]. Parameter τ_p is set equal to $\tau_p = \dfrac{h^2}{12\nu}$. The use of quadratic shape functions for velocities and linear interpolation for pressures, leading to a Taylor-Hood element which is *inf-sup* stable, would be the other choice. Though, in that case, no optimal definition of parameter τ_s exists [4].

3. DOMAIN DECOMPOSITION

3.1. Partitioning of the domain

In a mixed framework, the fluid domain is described as an assembly of subdomains and interfaces. Each of these components has its own variables and equations (equilibrium and behavior). Figure 1
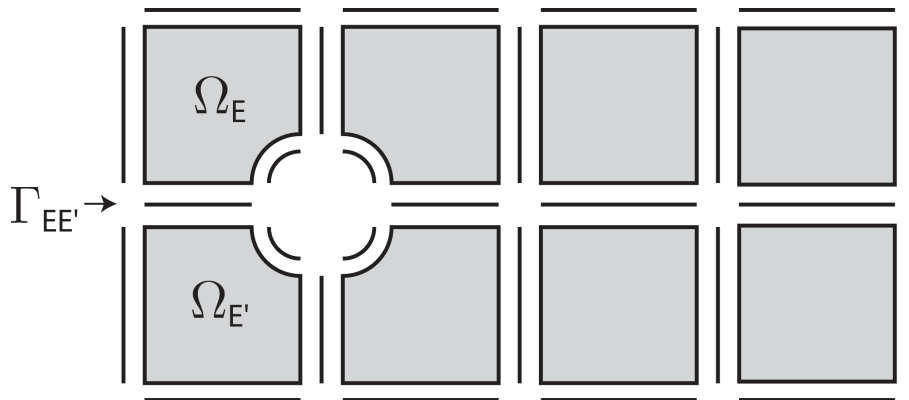

Fig. 1. Partitioning of the domain.

illustrates this decomposition. For the flow problem being considered, we choose to use the following variables: the velocity and pressure fields in the subdomains, and the velocity and force distributions at the interfaces.

3.2. Reformulation of the problem

Let the subscript $\square_E$ denote the restriction of any quantity $\square$ to a subdomain $\Omega_E, E \in \mathscr{E}$. Two subdomains Ω_E and $\Omega_{E'}$ are connected together by an interface $\Gamma_{EE'}$. The boundary $\partial \Omega_E$ connects Ω_E to the neighboring interfaces through the velocity and force distributions $\underline{W}_E$ and $\underline{F}_E$.

The equations of the subdomains are the Navier–Stokes equations. Concerning the admissibility of the interface quantities, $\underline{W}_E$ should be the projection of $\underline{v}_E$ onto $\partial \Omega_E$ and $\underline{F}_E$ should be statically admissible, i.e., $-p_E \underline{n} + 2\nu(\underline{n} \cdot \underline{\nabla}^S)\underline{v}_E = \underline{F}_E$.

Since we are only dealing with perfect internal interfaces, we should have continuity of the velocities and equilibrium of the forces over $\Gamma_{EE'}$, i.e. $\underline{W}_E = \underline{W}_{E'}$ and $\underline{F}_E + \underline{F}_{E'} = \underline{0}$. The interface concept can be extended to the external boundaries:

- Dirichlet boundary conditions can be expressed as $\underline{W}_E = \underline{v}_d$;

- Neumann boundary conditions result in $\underline{F}_E = \underline{f}$.

Then, the problem becomes:

Find $(\underline{v}_E, p_E, \underline{W}_E, \underline{F}_E)_{E \in \mathscr{E}}$ such that:

1. for all the subdomains

   (a) $(\underline{v}_E, p_E)$ are solutions of ((7)) over Ω_E

   (b) $\underline{W}_E = \underline{v}_E|_{\partial \Omega_E}$

   (c) $-p_E \underline{n} + 2\nu(\underline{n} \cdot \underline{\nabla}^S)\underline{v}_E = \underline{F}_E$

2. for all the interfaces

   (a) $\underline{W}_E = \underline{W}_{E'}$

   (b) $\underline{F}_E + \underline{F}_{E'} = 0$.

---

4. SINGLE-SCALE ITERATIVE STRATEGY

The reformulated problem 3.2 is solved using a two-stage iterative strategy; at Iteration $n+1$, one has to:

1. find $(\underline{v}_E, p_E, \underline{W}_E, \underline{F}_E)_{n+1}$ which verify the set of equations 1 along the search direction Z^-;

2. find $(\widehat{\underline{W}}_E, \widehat{\underline{F}}_E)_{n+1/2}$ which verify the set of equations 2 along the search direction Z^+.

4.1. Convergence criterion

The iterative process can be viewed as the search for solutions within two spaces alternatively: the linear space of the interface quantities defined by the interface relations, and the nonlinear space of the subdomain variables defined by the Navier–Stokes equations and the projection relations onto the boundaries. Starting from a solution in one space, we seek a subsequent solution in the other space by following the search direction Z^+ or Z^- (see Fig. 2). The solution of the problem is at the
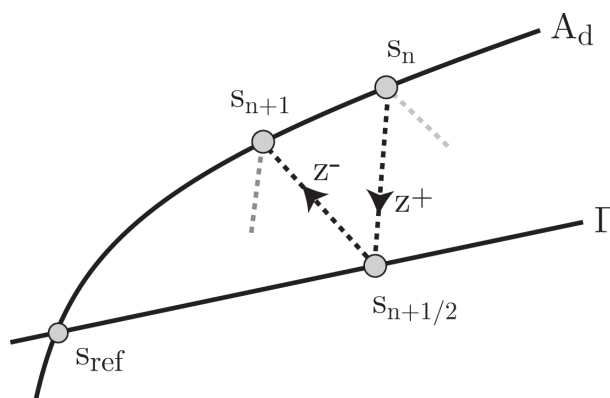
Fig. 2. Schematic representation of the iterative strategy.

intersection of the spaces, where it verifies all the equations. The convergence criterion is defined as the distance between the solutions $s_{n+1/2}$ and s_{n+1}:

$$\eta_{CR}^2 = \frac{\sum_{E\in\mathscr{E}} ||\underline{W}_E - \widehat{\underline{W}}_E||_{W,\partial\Omega_E}^2 + ||\underline{F}_E - \widehat{\underline{F}}_E||_{F,\partial\Omega_E}^2}{\sum_{E\in\mathscr{E}} ||\underline{W}_E + \widehat{\underline{W}}_E||_{W,\partial\Omega_E}^2 + ||\underline{F}_E + \widehat{\underline{F}}_E||_{F,\partial\Omega_E}^2},$$

$$||\square||_{W,\partial\Omega_E}^2 = \int_{\partial\Omega_E} \square \cdot \underline{\underline{z}}\square,$$

$$||\square||_{F,\partial\Omega_E}^2 = \int_{\partial\Omega_E} \square \cdot \underline{\underline{z}}^{-1}\square.$$

4.2. The subdomain stage at Iteration $n+1$

At this stage, we seek the velocities $\underline{W}_E^{n+1}$ and the forces $\underline{F}_E^{n+1}$ at the interfaces along with the velocity field $\underline{v}_E^{n+1}$ and the pressure field p_E^{n+1} within the subdomains, knowing the fields $\widehat{\underline{W}}_E^{n+1/2}, \widehat{\underline{F}}_E^{n+1/2}$ and the descent search direction Z^-. A subdomain's trial solutions and test functions are sought in the following spaces:

$$\underline{v}_E, \underline{w}_E \in \mathscr{V}_E = H^1(\Omega_E),$$

$$p_E, q_E \in \mathscr{Q}_E = L^2(\Omega_E),$$

$$\underline{W}_E \in \mathscr{V}_{\Gamma_E} = \left(H^1(\partial\Omega_E), \underline{W}_E = \underline{v}_E|_{\partial\Omega_E}\right),$$

$$\underline{W}_E^*, \underline{F}_E, \underline{F}_E^* \in \mathscr{V}_{\Gamma_E}^* = H^1(\partial\Omega_E).$$

The fields which are known at this stage are designated with a hat ($\widehat{\square}$), and the superscript $^{n+1}$ is omitted for the unknowns. Find $(\underline{v}_E, p_E, \underline{W}_E, \underline{F}_E)$ such that:

- $(\underline{F}_E - \widehat{\underline{F}}_E) + \underline{\underline{z}}(\underline{W}_E - \widehat{\underline{W}}_E) = 0$ over $\partial\Omega_E$

- $\underline{v}_E, p_E$ are Navier–Stokes solutions within Ω_E.

The search direction operator $\underline{\underline{z}}$ establishes a Robin condition for the whole boundary $\partial\Omega_E$. Parameter $\underline{\underline{z}}$ can be interpreted as the influence on Ω_E of its complementary part $\Omega \setminus \Omega_E$. The discussion on the search direction will continue in Subsec. 5.4.

In the weak form, the previous two equations together lead to:

Find $(\underline{v}_E, p_E, \underline{W}_E)_{E \in \mathscr{E}}$ such that $\forall \underline{w}, \underline{W}^* = \underline{w}|_{\partial \Omega_E}, q$:

$$\mathscr{A}_{\Omega_E}(\underline{v}, \underline{w}, p, q) + \left(\underline{\underline{z}} \underline{W}_E, \underline{W}^* \right)_{\partial \Omega_E} = (\underline{b}, \underline{w})_{\Omega_E} + \left(\widehat{\underline{F}}_E + \underline{\underline{z}} \widehat{\underline{W}}_E, \underline{W}^* \right)_{\partial \Omega_E}. \tag{8}$$

Problem (8) is nonlinear and is solved by the Newton-Raphson method with SUPG and PSPG stabilization.

4.3. The interface stage at Iteration $n + 1/2$

The interfaces connect subdomains to one another or to the boundaries through mixed force and velocity distributions. Each internal interface has two sides whose quantities are denoted $\square$ and $\square'$. The external interfaces (at the boundary of the domain) have only one side on which only $\square$ exists. At the interface stage, we designate the unknowns with a hat $(\widehat{\square})$.

4.3.1. Search directions

The search directions are parameters of the method which connect the solutions within the subdomains and at the interfaces. Here, the search direction Z^+ at the interface stage writes:

$$\widehat{\underline{F}} - \underline{F} - \underline{\underline{z}}(\widehat{\underline{W}} - \underline{W}) = 0.$$

The operator $\underline{\underline{z}}$ is a parameter of the method. It acts on the interface fields, but does not couple the normal and tangential components together. Thus, for a given interface with the normal $\underline{n}$, it can be written as

$$\underline{\underline{z}} = z_n \underline{n} \otimes \underline{n} + z_t (\underline{\underline{I}} - \underline{n} \otimes \underline{n}).$$

When this type of domain decomposition is applied to subdomains with linear elastic material law, optimum expressions of the search directions can be obtained. In the present case, two parameters z_n and z_t express different impedances in the normal and tangent directions.

4.3.2. Calculation of the interface fields

Perfect interfaces. Perfect interfaces have two sides (each with a search direction) and two behavior laws. Since the search directions are local operators in space and the equations are verified in a weak sense, one gets four point-wise relations leading to the following system:

$$\mathbb{A} \widehat{Q} - \begin{bmatrix} \underline{F} - \underline{\underline{z}} \underline{W} \\ \underline{F}' - \underline{\underline{z}} \underline{W}' \end{bmatrix} = 0,$$

with $\widehat{Q} = [\widehat{\underline{F}}, \underline{\underline{z}} \widehat{\underline{W}}]^T$ and $\mathbb{A} = \begin{bmatrix} 1 & -1 \\ -1 & -1 \end{bmatrix}$, whose solution is

$$\widehat{\underline{W}} = \widehat{\underline{W}}' = \frac{1}{2}(\underline{W} + \underline{W}') + \frac{1}{2} \underline{\underline{z}}^{-1}(\underline{F} + \underline{F}'),$$

$$\widehat{\underline{F}} = -\widehat{\underline{F}}' = \frac{1}{2}(\underline{F} - \underline{F}') - \frac{1}{2} \underline{\underline{z}}(\underline{W} - \underline{W}').$$

Boundary conditions. Dirichlet and Neumann interfaces have only one side and two unknowns. Similarly, one gets:

$$\widehat{\underline{W}} = \underline{W}_d,$$

$$\widehat{\underline{F}} = \underline{F} + \underline{\underline{z}}(\underline{W}_d - \underline{W}),$$

for a prescribed velocity Interface and

$$\widehat{\underline{F}} = \underline{F}_d,$$

$$\widehat{\underline{W}} = \underline{W} + \underline{\underline{z}}^{-1}(\underline{F}_d - \underline{F}),$$

for a prescribed traction Interface.

Example: Poiseuille flow. Let us consider an established flow between two plates along a length $L = n \times l$, where n is the number of subdomains used in the simulation and $l = 0.2$ m. $H = 1$ m is the distance between the plates. The prescribed velocity is parabolic, with $\underline{v}_d = U\dfrac{4y(H-y)}{H^2}\underline{e}_x$.
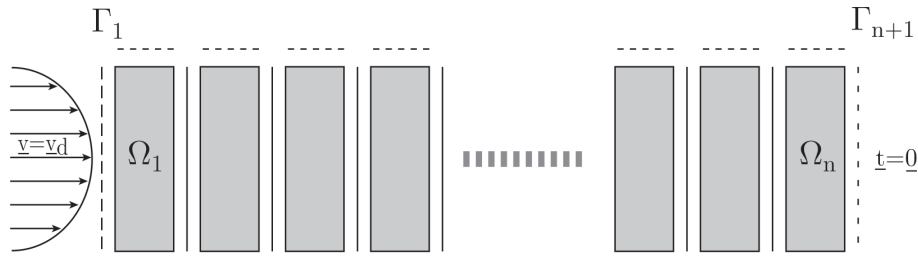
Fig. 3. Decomposition of the Poiseuille flow problem.

For this very simple problem, where the non-linear convective term plays vanishes in the momentum equation, the obtained results are not satisfying. The domain decomposition method we proposed, without scale separation, leads to a convergence rate which depends on the number of subdomains, as shown in Fig. 4. It can be easily argued that for more complex problems, the performances would probably be worse.
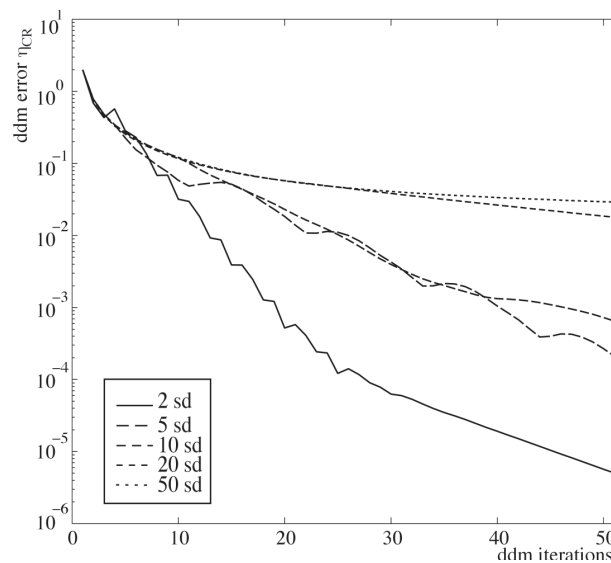

Fig. 4. The error indicator as a function of the number of iterations for the domain decomposition method without scale separation.

5. THE MACROPROBLEM BASED ON GLOBAL VOLUME CONSERVATION

Domain decomposition methods need a global problem to maintain the same convergence rate with increasing number of subdomains. In some methods, the global problem is the interface problem based on the Lagrange multipliers. In the LaTIn family of methods, a macroproblem is defined, based on equilibrium of forces and moments and continuity of displacements at a macroscopic scale. The macroscopic quantities are defined by chosing a basis on each interface (for example, constant and linear components) and can be adapted to the problem at hand (a basis containing discontinuous function is used for crack propagation [8]). Here, we propose an original macroproblem for incompressible flows. On the basis of global volume conservation, we introduced a macroproblem in order to enable rapid propagation of the information to the whole set of subdomains. Two ways of building this problem, both based on the fact that for an incompressible flow $\underline{\nabla} \cdot \underline{v} = 0$ in V, led to different efficiencies. At convergence, $\widehat{\underline{W}}_E = \underline{W}_E = \underline{v}_E|_{\partial\Omega_E}$, therefore:

$$\int_{\partial\Omega_E} \widehat{\underline{W}} \cdot \underline{n} \, \mathrm{d}S = 0 \quad \forall E \in \mathscr{E}, \tag{9}$$

$\underline{n}$ being the outward unit normal to Subdomain Ω_E. $\underline{n}$ is defined locally, for each element of $\partial\Omega_E$. Equation (9) involves only velocity averages, $i.e.$, macroparts $(^M)$ as defined below:

$$\underline{\square}^M = \square^M \underline{n}_0 = \frac{1}{mes(\Gamma)} \int_\Gamma \underline{\square} \cdot \underline{n}_0 \, \mathrm{d}S \, \underline{n}_0,$$

$$\underline{\square} = \square^M \underline{n}_0 + \underline{\square}^m,$$

$\underline{n}_0$ is a unit normal to Interface Γ. Two normals to Interface Γ have already be defined: $\underline{n}$ pointing outwards Ω_E and $\underline{n}'$ pointing outwards $\Omega_{E'}$. Choosing $\underline{n}_0$ corresponds to choosing a preferred orientation of the normal, it can be $\underline{n}$ or $\underline{n}'$ indifferently, but one has to keep in mind that $\underline{n}_0$ is a locally defined unit normal vector, that is defined for each element of Interface Γ. The complementary micropart $\widehat{\underline{W}}^m = \widehat{\underline{W}} - \widehat{\underline{W}}^M$ is not involved in (9). We enforce this macroequation at each iteration. The first macroproblem is a projection of $\widehat{\underline{W}}$ onto the space defined by (9). The second macroproblem involves both the macrovelocities and macroforces while relaxing the search directions. The proposed scale separation enables us to have a macroproblem with only one unknown per field, making it very small.

5.1. Uncoupling of the micro and macro parts

The microparts and macroparts of the interface fields belong to two orthogonal spaces:

$$\int_\Gamma \widehat{\underline{W}} \cdot \widehat{\underline{F}} \, \mathrm{d}S = \mathrm{mes}(\Gamma)\widehat{W}^M \widehat{F}^M + \int_\Gamma \widehat{\underline{W}}^m \cdot \widehat{\underline{F}}^m \mathrm{d}\,S,$$

$$\text{thus:} \quad (\widehat{\underline{W}}, \widehat{\underline{F}})_\Gamma = (\widehat{\underline{W}}^M, \widehat{\underline{F}}^M)_\Gamma + (\widehat{\underline{W}}^m, \widehat{\underline{F}}^m)_\Gamma.$$

5.2. Least-squares solution

Using the interface fields calculated as described in Subsubsec. 4.3.2, we build new macrovelocities B^M:

Find B^M which makes stationary the Lagrangian:

$$\sum_i \frac{1}{2} \int_{\Gamma_i} (B^M - \widehat{W}^M)^2 \, \mathrm{d}S + \sum_{E \in \mathscr{E}} \mu_E \int_{\partial\Omega_E} B^M \underline{n}_0 \cdot \underline{n} \, \mathrm{d}S.$$

In order to do that, we set fixed velocities along $\partial_{\underline{v}}\Omega$ and modify the velocities of the internal interfaces and of the interfaces with prescribed tractions. This problem does not modify the interface force fields $\widehat{\underline{F}}$ and does not improve the domain decomposition method, as shown in Fig. 5 for the Poiseuille flow problem. Only, the slight oscillations on the curves in Fig. 4 have disappeared.
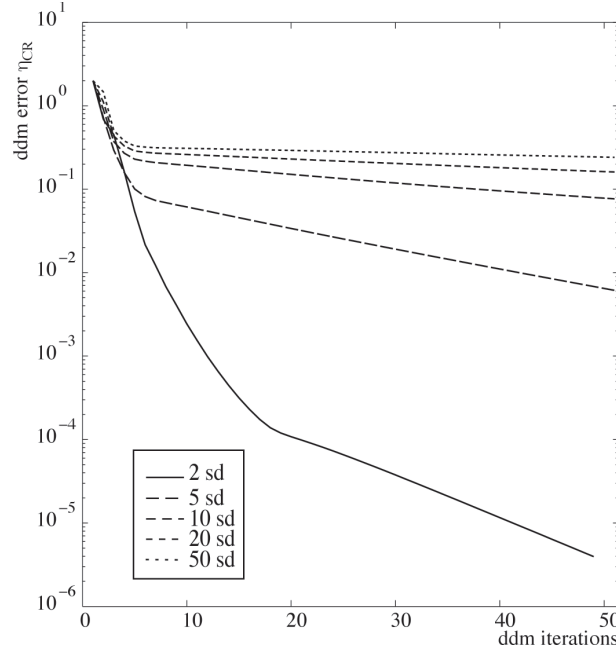

Fig. 5. Error indicator as a function of the number of iterations for the first macroproblem.

5.3. Relaxation of the search direction

In a weak sense, the search direction equation for the macroparts can be written as: find $\widehat{F}^M, \widehat{W}^M$ such that $\forall\, \widehat{W}^{M*}$:

$$\sum_{E\in\mathscr{E}}\int_{\partial\Omega_E}\left(\left(\widehat{F}^M - F^M\right) - z_n(\widehat{W}^M - W^M)\right)\widehat{W}^{M*} = 0, \tag{10}$$

with the constraint from the macroproblem

$$\int_{\partial\Omega_E}\widehat{\underline{W}}^M\cdot\underline{n}\,\mathrm{d}S = 0\qquad \forall E\in\mathscr{E}.$$

This constraint is enforced via a Lagrange multiplier μ_E for each subdomain:

find $\widehat{F}^M, \widehat{W}^M, \mu_E$ such that:

$$\sum_{E\in\mathscr{E}}\int_{\partial\Omega_E}\left(\left(\widehat{F}^M - F^M\right) - z_n(\widehat{W}^M - W^M)\right)\underline{n}_0\cdot\widehat{W}^{M*}\underline{n}_0 + \mu_E\widehat{W}^{M*}\underline{n}_0\cdot\underline{n} = 0 \quad \forall\,\widehat{W}^{M*},$$

$$\sum_{E\in\mathscr{E}}\mu_E^*\int_{\partial\Omega_E}\widehat{W}^M\underline{n}_0\cdot\underline{n} = 0\qquad \forall\,\mu_E^*.$$

The previous equations are written in vector form. Indeed, the scale separation is dependent on the choice of a preferred normal orientation $\underline{n}_0$ for each interface. Volume conservation is expressed

by looking outwards from the subdomains, *i.e.*, by using $\underline{n}$. Considering a particular interface and assuming, for example, that $\underline{n} = \underline{n}_0 = -\underline{n}'$ for each element of $\partial\Omega_E$ leads to the following system:

$$(\widehat{F}^M - F^M) - z_n(\widehat{W}^M - W^M) + \mu_E\underline{n} \cdot \underline{n}_0 = 0,$$
$$(\widehat{F'}^M - F'^M) - z_n(\widehat{W'}^M - W'^M) + \mu_{E'}\underline{n}' \cdot \underline{n}_0 = 0,$$

with the interface behavior, one gets

$$(\widehat{F}^M - F^M) - z_n(\widehat{W}^M - W^M) + \mu_E = 0,$$
$$(-\widehat{F}^M - F'^M) - z_n(\widehat{W}^M - W'^M) - \mu_{E'} = 0.$$

Boundary conditions. In the particular case of interfaces involving boundary conditions, one gets

$$(\widehat{F}^M - F^M) - z_n(\widehat{W}^M - W^M) + \mu_E = 0.$$

The prescribed conditions $(\widehat{W}^M = \widehat{W}_d^M$ or $\widehat{F}^M = \widehat{F}_d^M)$ define the admissibility spaces of the macroquantities. Thus, there is only one equation in the macroproblem for each boundary condition interface.

Poiseuille flow. The second formulation of the macroproblem enables rapid propagation of the pressure and velocity information. During the first iteration, a pressure gradient is already established in the whole domain and the magnitude of the velocity is much closer to the value at convergence. The delayed exchanges of forces and velocities encountered with the version of the macroproblem described (Subsec. 5.2) previously no longer occur, which makes the method very efficient. Indeed, the convergence rate does not depend on the number of subdomains in the problem. Figure 6 shows clearly that regardless of the number of subdomains the same level of error is reached for a given number of iterations.
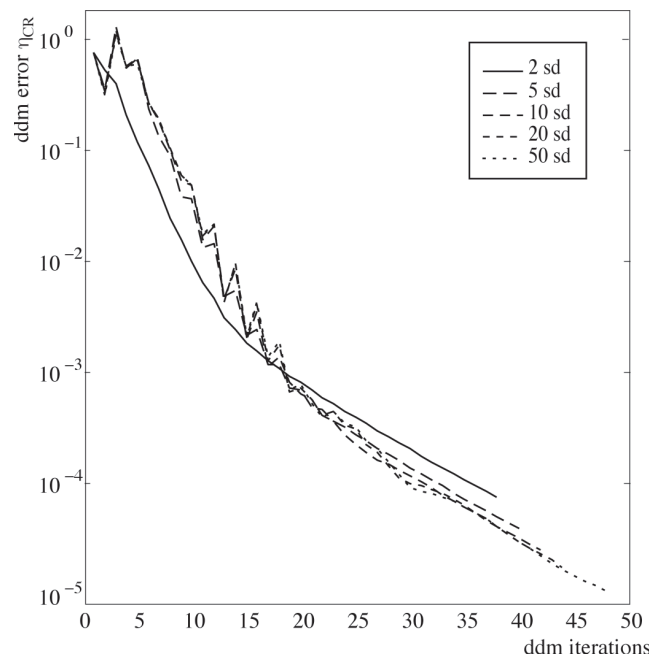

Fig. 6. The error indicator as a function of the number of iterations for the second macroproblem.

5.4. Influence of the search directions

After studying the influence of Parameter z_n on the convergence rate, we observed the existence of one optimum parameter (*i.e.*, one which achieves the smallest error at a given iteration) for each problem.

The search direction has the dimension $\rho\nu/L$. The Poiseuille flow problem was solved for various values of the viscosity ν, the prescribed velocity U and the characteristic length $L = H$ (which is the length between the two plates). Figure 7 shows that the convergence of the iterative process was faster in the range $[5\rho\nu/L, 50\rho\nu/L]$. Therefore, we chose this range for subsequent search directions. This optimum range does not depend on the prescribed velocity.
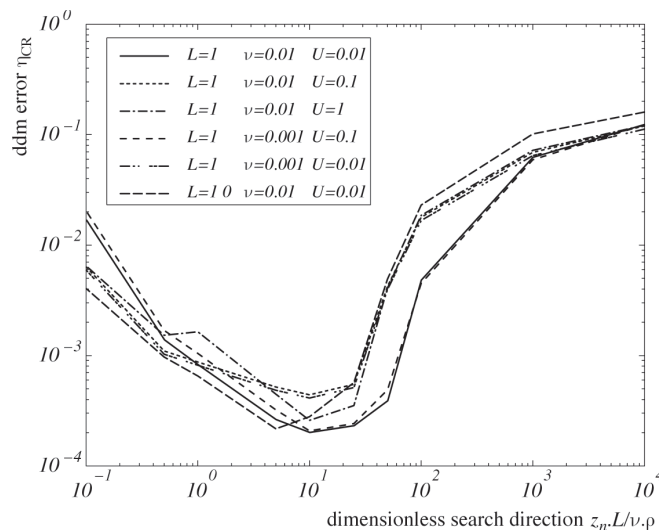
Fig. 7. The error η_{CR} as a function of the dimensionless search direction in various cases.

The method should now be tested on more complex examples, involving non-linearity and time dependence.

6. EFFICIENCY OF THE METHOD

6.1. Benchmark 1: 2D flow around a fixed cylinder

Problem statement. The benchmark proposed by Schäfer and Turek [15] enables us to compare our results with reference results in order to assess the quality of the numerical resolution of the fluid flow problem. This 2D test case concerns the simulation of the flow past a circular cylinder of diameter $D = 0.1$ inside a channel of width $H = 0.41$ and length $L = 2.2$. The inflow boundary condition is a prescribed parabolic velocity and the outflow corresponds to a zero prescribed traction condition. The geometry of the problem is shown in Fig. 8. For the stationary case, the inflow condition is parabolic (11).

$$v_d = U_{\max} \times \frac{4y(H - y)}{H^2} \qquad U_{\max} = 0.3. \tag{11}$$

The viscosity is $\nu = 10^{-3}$ m^2/s and the density is $\rho = 1$ kg/m^3. The Reynolds number is defined by $\mathscr{R}_e = U_\infty D/\nu$, $U_\infty = 2U_{\max}/3$. The drag and lift coefficients are defined from the resultants of the forces applied to the cylinder:

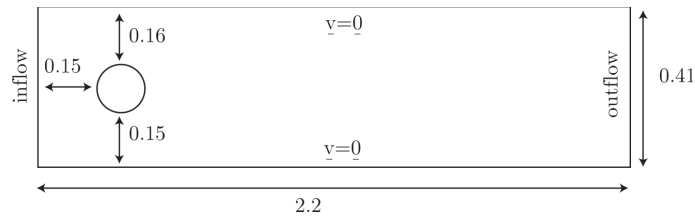$$c_D = \frac{2F_D}{\rho D U_\infty^2}, \qquad c_L = \frac{2F_L}{\rho D U_\infty^2}.$$

Fig. 8. Geometry of the benchmark.

Results for stationary flow. When the Reynolds number is set to $\mathscr{R}_e = 20$, the flow is known to be stationary, so we drop the time derivative term in the momentum equation, and change the stabilization parameter τ_s consequently. Figures 9 and 10 show the fields calculated by the domain
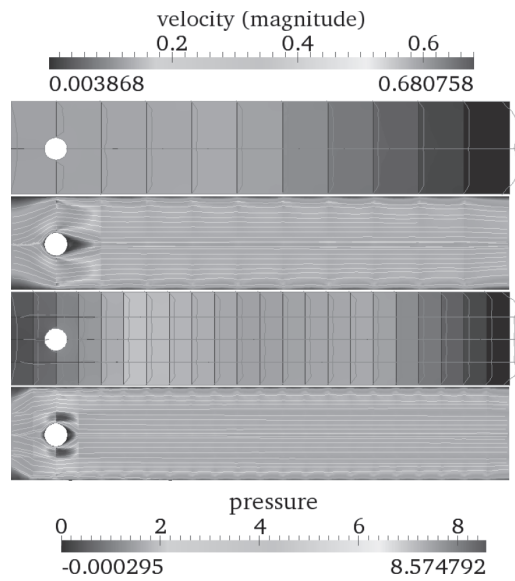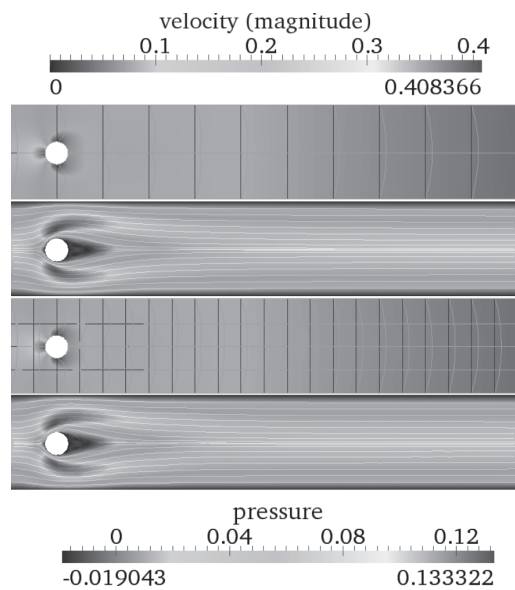

Fig. 9. Calculated fields: pressure (top) and velocity (bottom) at Iteration 1. The interfaces are wrapped by the velocity field and pictured in grey. Twenty-two and 88 subdomains were used.

Fig. 10. Calculated fields: pressure (top) and velocity (bottom) at Iteration 15. The interfaces are wrapped by the velocity field and pictured in grey. Twenty-two and 88 subdomains were used.

decomposition method using 22 (top) and 88 (bottom) subdomains and the second macroproblem previously described (Subsec. 5.3). Pressure and velocity fields are depicted with associated color scales, as well as streamlines, interfaces of the domain decomposition and velocity profile on the interfaces. It can be seen that as soon as Iteration 1 take place the flow develops in the whole domain. Results at Iteration 15 are shown for visual evaluation of what $\eta_{CR} \leq 10^{-3}$ achieves. The associated convergence results are shown in Fig. 11. One can see that the macroproblem enables faster convergence. With 22 subdomains, it can be seen that the convergence is anyhow faster. However, for the first 15 iterations the slope is the same. At iteration 15, the error indicator is less than 10^{-3}. For the remaining part of the iterations, the 88-subdomain decomposition is disadvantaged, due to the presence of interfaces in the recirculation zone. This local phenomenom is not captured by the macroproblem, yielding slower convergence.
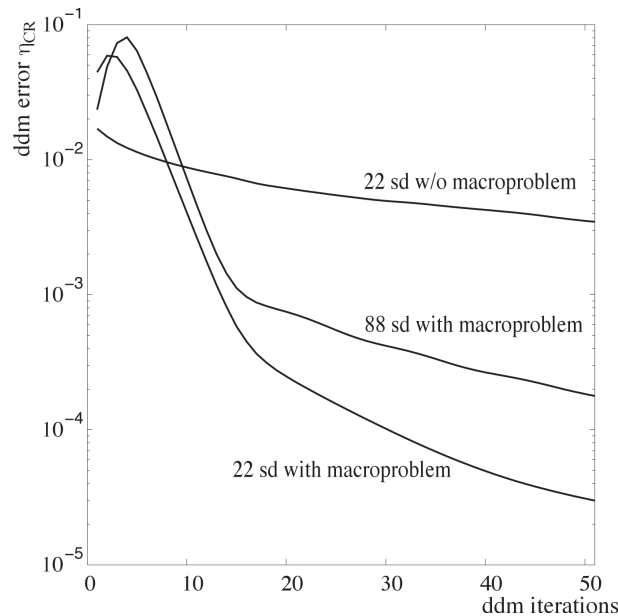

Fig. 11. The error as a function of the number of iterations for the stationary flow around a cylinder.

Drag and lift coefficients. Here, a lift coefficient of 0.015 and 0.013 and a drag coefficient of 5.64 and 5.65 are computed with 22 and 88 subdomains, respectively. This is in agreement with the results reported in [15] which range from 0.014 to 0.011 and from 5.57 to 5.59, respectively. Nevertheless, considering that less than 35,000 unknowns were employed, these results cannot be considered so bad. The recirculation length is of 0.85 and pressure drop 0.12 which is again in good accordance with reference results ([0.842, 0.852] and [0.1172, 0.1176], respectively).

6.2. Benchmark 2: flow across a square cavity

A question that arises is how the method behaves when using interfaces that are not either parallel or orthogonal to the main direction of the flow. Let us consider a square decomposed into 10×10, 7×7 or 5×5 square subdomains, each with 10 elements in the x and y directions. The boundary conditions are a prescribed parabolic horizontal velocity over the bottom left interface, and free outflow over the upper right interface, as represented in Fig. 12. Maximum velocity is 0.3, viscosity is 10^{-2}, leading to Reynolds number $\mathscr{R}_e = 30$. This test case illustrates the method when domain decomposition interfaces are of arbitrary orientation with respect to the flow field. Figure 13 shows the evolution of the error indicator as a function of the number of iterations for the three decompositions. One can judge that the method performs identically for each decomposition. Figure 14 shows the computed velocity (with streamlines) and pressure fields at Iterations 1, 3, 5, 7 and 9 with 100 subdomains.
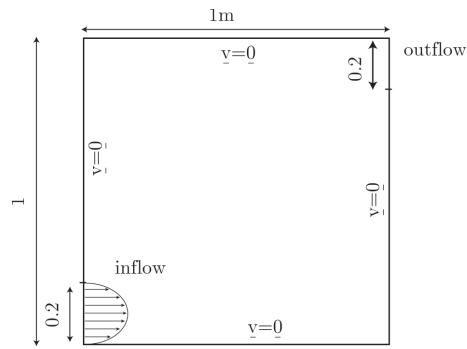
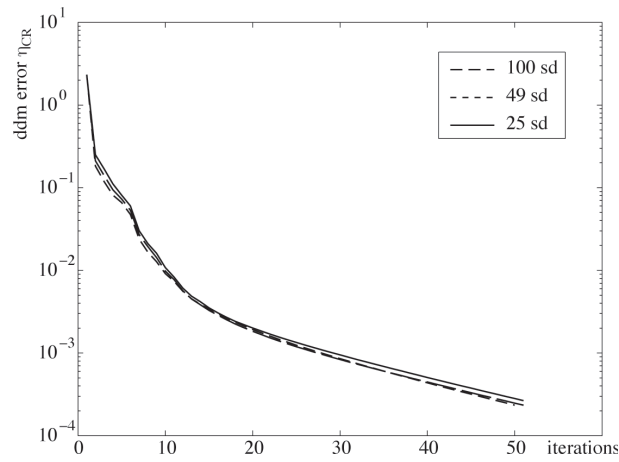**Fig. 12.** Problem setup for the square cavity.

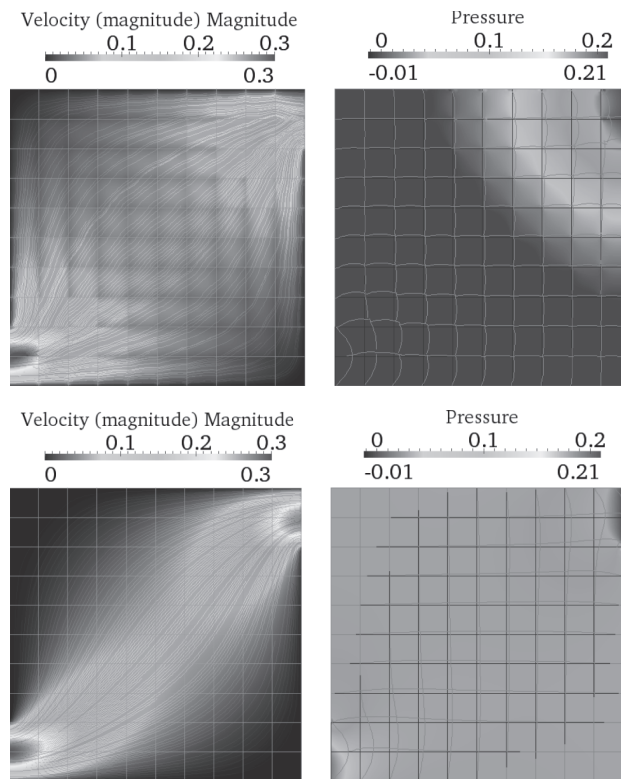**Fig. 13.** The error indicator as a function of the number of iterations for the square problem.

Fig. 14. Calculated fields: velocity (left) and pressure (right) at Iterations 1 (top) and 20 (bottom) for 10×10 subdomains. The interfaces are wrapped by the velocity field and pictured in grey.

6.3. Benchmark 3: Non-stationary flow around a cylinder

When set to 100, the Reynolds number reflects a transient flow. Periodic vortex shedding occurs in the cylinder's wake. The problem is no longer stationary, and we use a Crank-Nicholson time integration scheme. At each time step, the Navier–Stokes problem is solved by the proposed multiscale method. The SUPG stabilisation parameter has to be adapted to:

$$\tau_{\text{SUPG}} = \left(\frac{2}{\Delta t} + \frac{2||\underline{v}||}{h} + \frac{4\nu}{h^2} \right)^{-1}.$$

The time step is set to $\Delta t = 20$ ms and the initial condition is a fluid at rest ($\underline{v} = \underline{0}$, $p = 0$). The flow is progressively raised from $U_{\text{max}} = 0$ to $U_{\text{max}} = 1.5$ over 50 time steps. The computation then goes on for seven seconds.

We can see from Fig. 15 that the expected periodic vortex shedding occurs behind the cylinder. Figure 16 shows the drag and lift coefficients on the cylinder. The vortex shedding is pseudo-periodic, after a transition period of five seconds. A Strouhal number can be extracted from Fig. 16. It is defined from the frequency of the oscillations of the lift coefficient by

$$S_t = \frac{Df}{2U_{\text{max}}/3}.$$

With a Fourier transformation of the lift coefficient, the Strouhal number is evaluated at $S_t = 0.293$, within 1% from the value reported in [15].
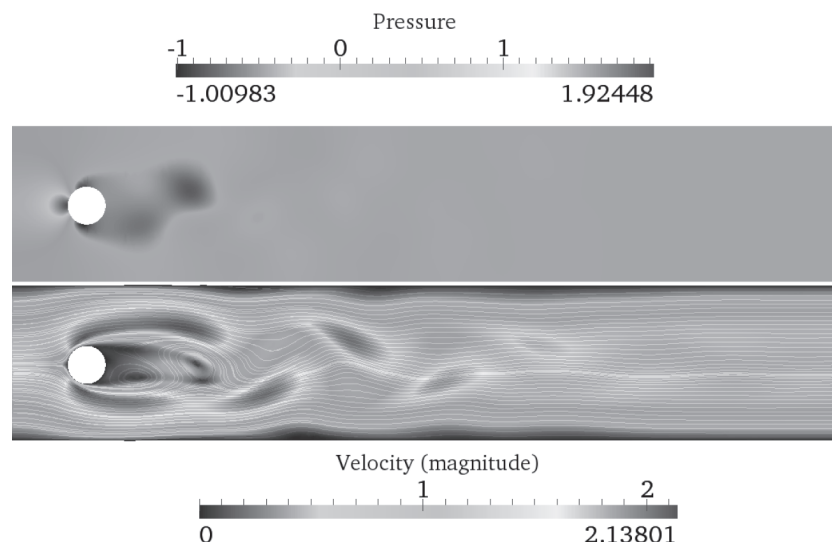

Fig. 15. Pressure and velocity magnitude at time $t = 8$ s, using 88 subdomains. Streamlines are represented over the velocity field.
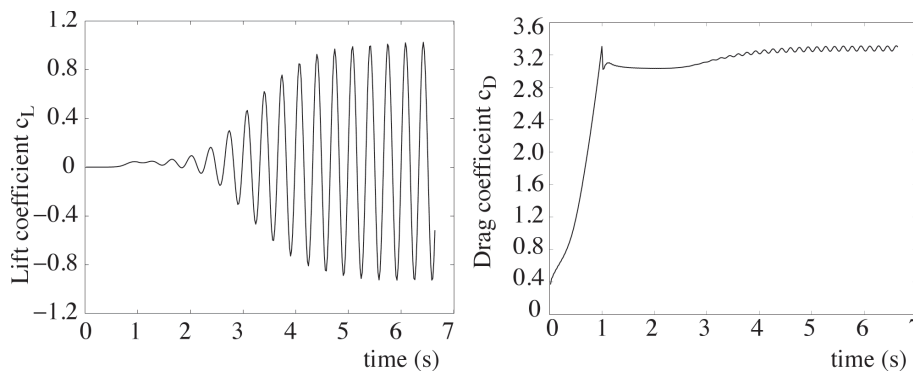

Fig. 16. Calculated lift and drag coefficients for time between 0 and 8 s, using 88 subdomains.

7. Conclusion

This paper presents a domain decomposition method dedicated to the incompressible flow of viscous fluids governed by the Navier–Stokes equations. The mixed Framework used at the interface level allows to formulate the interface connection problem both for the continuity and equilibrium conditions. The non-linear problems on the subdomain level are solved by a finite element method with appropriate stabilizations. The integral form of the divergence-free velocity field condition on each sub-domain allows to build a very small global interface problem whose aim is to improve the scalability of the method. The later involves two unknowns per interface only, which leads to nearly no additional numerical cost. First, we attempted to solve this problem using a least-squares algorithm, but did not achieve the expected level of performance because this approach does not account for the pressure macroquantities. Then, by enforcing the constraints at the macroscopic level using a Lagrange multiplier in each search direction equation, we ended up with an efficient macroproblem resulting in rapid propagation of the macroquantities throughout the computational domain. The domain decomposition method using this macroproblem has a good numerical scalability even though when interfaces are used in areas prone to strong recirculation the convergence rate depends on the number of subdomains used in the calculations. Therefore, we are working on the possibility to slightly adapt the macrobasis in those regions.

References

[1] S. Behara, S. Mittal. Parallel finite element computation of incompressible flows. *Parallel Comput.*, **35**: 195–212, 2009.
[2] Chacón Rebollo, Tomás and Chacón Vera, Eliseo. Study of a non-overlapping domain decomposition method: Steady Navier–Stokes equations. *Applied Numerical Mathematics*, **55**(9): 100–124, 2005.
[3] V. Dolean and S. Lanteri. Parallel multigrid methods for the calculation of unsteady flows on unstructured grids: algorithmic aspects and parallel performances on clusters of PCS. *Parallel Computing*, **30**: 503–525, 2004.
[4] J. Donea, A. Huerta. Finite Element Methods for Flow Problems. *ed. Wiley*, 2003.
[5] C. Farhat, F.-X. Roux. A method of finite element tearing and interconnecting and its parallel solution algorithm. *IJNME*, **32**: 1205–1227, 1991.
[6] R. Glowinski, T.W. Pan, J. Periaux. *Fictitious domain/domain decomposition methods for partial differential equations*. Domain-based parallelism and problem decomposition method in computational science and engineering, pp. 177–192, Philadelphia, 1995.
[7] Volker Gravemeier, Wolfgang A. Wall, Ekkehard Ramm. A three-level finite element method for the instationary incompressible Navier–Stokes equations. *Computer Methods in Applied Mechanics and Engineering*, **193**(15–16): 1323–1366, 2004.
[8] P.-A. Guidault, O. Allix, L. Champaney, C. Cornuault. A multiscale extended finite element method for crack propagation. *Computer Methods in Applied Mechanics and Engineering*, **197**(5): 381–399, 2008.
[9] T.J.R. Hughes, G.R. Feijóo, L. Mazzei, J-B. Quincy. The variational multiscale method: a paradigm for computational mechanics. *Computer Methods in Applied Mechanics and Engineering*, **166**: 3–24, 1998.
[10] P. Ladevèze. Multiscale modelling and computational strategies for composites. *International Journal for Numerical Methods in Engineering*, **60**(1): 233–253, 2004.
[11] P. Ladevèze, D. Dureissex. A new micro-macro computational strategy for structural analysis. *Compte-rendu de l'académie des sciences*, **337 IIB**: 1327–1344, 1999.
[12] J. Li. Dual primal FETI methods for stationary stokes and Navier–Stokes equations, 2002.
[13] J.Mandel. Balancing domain decomposition. *Communications in Applied Numerical Methods*, **9**: 233–241, 1993.
[14] C.A. Rivera, M. Heniche, R. Glowinski, P.A. Tanguy. Parallel finite element simulations of incompressible viscous fluid flow by domain decomposition with Lagrange multipliers. *J. Comput. Phys.*, **229**: 5123–5143, 2010.
[15] M. Schäfer, S. Turek. Benchmark computations of laminar flow around a cylinder. *Flow Simulation with High-Performance Computation II*, **52**: 547–566, 1996.
[16] Y.Q. Shang, Y.N. He.Parallel finite element algorithms based on full domain partition for stationary Stokes equations. *Appl. Math. Mech.-Engl. Ed.*, **31**(5): 643–650, 2010.

[17] Y.Q. Shang, Y.N. He.Parallel iterative finite element algorithms based on full domain partition for the stationary Navier–Stokes equations. *Appl. Numer. Math.*, **60**(7): 719–737, 2010.

[18] T.E. Tezduyar, S. Mittal, S.E. Ray, R. Shih. Incompressible flow computations with stabilized bilinear and linear equal-order-interpolation velocity-pressure elements. *Computer Methods in Applied Mechanics and Engineering*, **95**(2): 221–242, 1992.

[19] A. Toselli. FETI domain decomposition methods for scalar advection-diffusion problems. *Computer Methods in Applied Mechanics and Engineering*, **190**(43–44): 5759–5776, 2001.

[20] U. Trottenberg, C.W. Oosterlee, A. Schuller. *Multigrid*. Academic Press, 2001.

[21] B. Vereecke, H. Bavestrello, D. Dureisseix. An extension of the FETI domain decomposition method for incompressible and nearly incompressible problems. *Comput. Methods Appl. Mech. Eng.*, **192**: 3409–3429, 2003.

[22] E. Vergnault, O. Allix, S. Maison-le-Poëc.Fluid-structure interaction with a multiscale domain decomposition method. *European Journal of Computational Mechanics*, **19**(1-2-3): 267–280, 2010.

[23] O.C. Zienkiewicz, R.L. Taylor, P. Nithiarasu. The Finite Element Methods for Fluid Dynamics. *ed. Butterworth-Heinemann*, 2005.